

# Correlating HALT & HASS, RS/HALT Vibration and End-Use Environments

Stephen A. Smithson, Smithson & Associates, Edina, Minnesota

Overcoming decades of shortcomings, applying a fatigue damage spectrum (FDS) to random shock (RS) machines used in HALT (highly accelerated life tests) and HASS (highly accelerated stress screening) provides improved usability and analysis results. FDS expands the benefits of HALT to benchmarking random shock (RS) excitations and product responses to correlate them with end-use-environments (EUE) and electrodynamic (ED) shakers thus quantifying severities of different excitations. It also addresses “What are you doing to my product?”; “When do I “Stop HALTING?” and more. FDS is a tool for test compression and documenting progress toward reliability and confidence goals.

The relative and cumulative fatigue damage metric for RS machines does not rely on the processing limitations of Gaussianity, stationarity, averaging of FFTs, loss of peaks while accommodating strongly mixed signals not addressed with traditional PSD and  $g_{\text{rms}}$  metrics. To be of value, the FDS metric should be a spectrum with frequency resolution that applies to *all* shaker types and EUE excitations and product responses. It can be shown that excitations of greatly different peak probability distributions (PPDs) produce identical PSDs and  $g_{\text{rms}}$  measurements. Thus the fatigue damage spectrum will be shown to better represent the severity of the excitation.

## Background

For almost 30 years, a limited definition and purpose of the HALT process, “stimulate it, break it, fix it” has prevailed. Acknowledging “stimulate not simulate” and the feedback and corrective action components, many users are left without the ability to relate the process, the test levels and the results to any other environments the product might see.<sup>5</sup> The traditional use of PSD ( $g^2/\text{Hz}$ ) and  $g_{\text{rms}}$  lacks elements that correlate to failure mode, fatigue cycles, and field exposure especially with amplitudes more severe than Gaussian. The PSD does not lead in a straightforward manner to the reliability and confidence numbers many users strategically seek from the HALT process. Because the PSD is a statistical snapshot of a random process, it is independent of time and fatigue cycles. Further, the FFT-generated PSD is neither mathematically nor practically valid for the non-Gaussian, non-stationary excitations of random shock (RS) machines.

## Kurtosis Primer

Kurtosis is the fourth statistical moment about the mean of a data set. The mean is the first, the standard deviation the second and skewness the third. Kurtosis describes the “peakiness” of the data and is described by the tails of the PPD and reflects a higher incidence of higher peak amplitudes than a Gaussian (normal) distribution.

Documented in John and Phil Van Baren’s studies and papers,<sup>3</sup> the tails of the PPD extend beyond the Gaussian normal with increased kurtosis. As shown in Figure 1, this translates to more time at the higher peaks and is quantified by increased cumulative damage for a field exposure.

When looking at data, the peak acceleration is easiest to identify and its ratio to the mean is the crest factor. Figure 2 indicates that a kurtosis of 3 for Gaussian random corresponds to a crest factor of 4.5 to 5, meaning peaks are 4.5 to 5 times the mean, even for Gaussian.

It is also important to remember that the crest factor is a simple ratio of a single peak to RMS level for a data set, while kurtosis relates all events in the PPD to the RMS level, or a measure of severity for the entire data set.

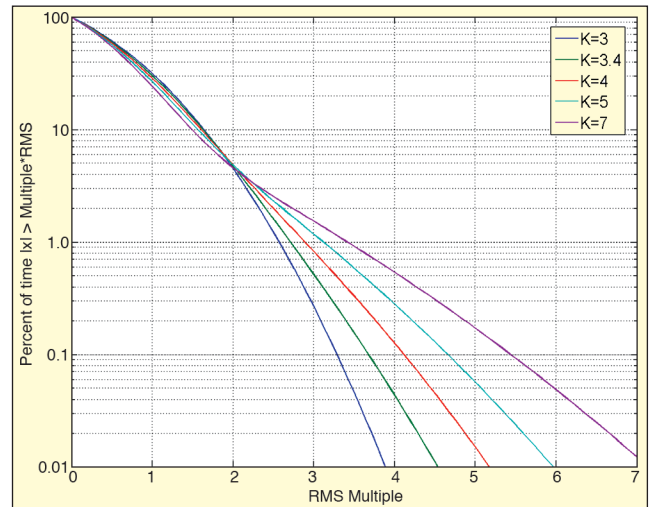


Figure 1. Increased kurtosis means more time at peaks. Kurtosis = 3 is  $> 3\sigma$  0.27% of time; kurtosis = 4 is  $> 3\sigma$  0.83% of time; kurtosis = 7 is  $> 3\sigma$  1.5% of time; 1.5% of a 1-hour test is nearly a minute above  $3\sigma$ .

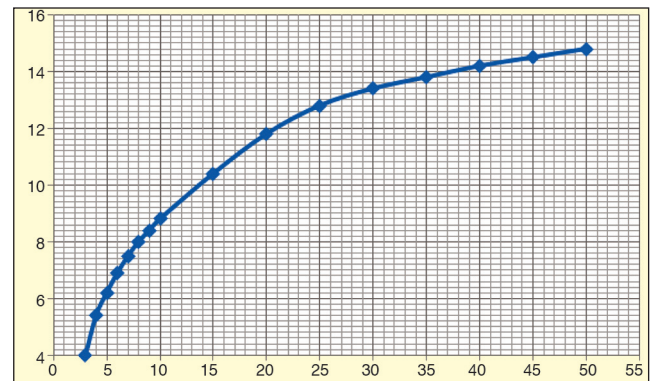


Figure 2 Kurtosis vs. crest factor (kurtosis of 3 yields 4-4.5  $\sigma$  peaks).

## Caveats

- RS machines RS1, RS2 and RS3 recorded for this exercise are from different manufacturers, vintages and designs. Their common feature is a 48 × 48-inch table. This evaluation is *not* a competitive comparison of RS machine designs or manufacturers, but FDS could be used for such. FDS demonstrates a better method for quantifying long-ignored relationships.
- RS control was on the table bottom for RS1 and RS2 and near the table top center for RS3.
- Both the PSD and the FDS lose relationships of phase and ordering of stress cycles, so FDS is *not* a replication, though it does yield an equivalent damage excitation.
- FDS is a means of generating a statistically more accurate test based on cumulative damage from multiple field exposures.
- Summing PSDs using enveloping or a MIL-SPEC formula still relies on PSD and  $g_{\text{RMS}}$  shortcomings.

As illustrated in Figure 3, an important advantage of the FDS is the ability to relate excitations of RS/HALT machines to end-use environments, time histories, ED shakers and specification test exposures such as those shown in Figure 4.

Whether for control or comparative analysis of severity, the FDS metric must be a spectrum with selectable frequency bandwidth

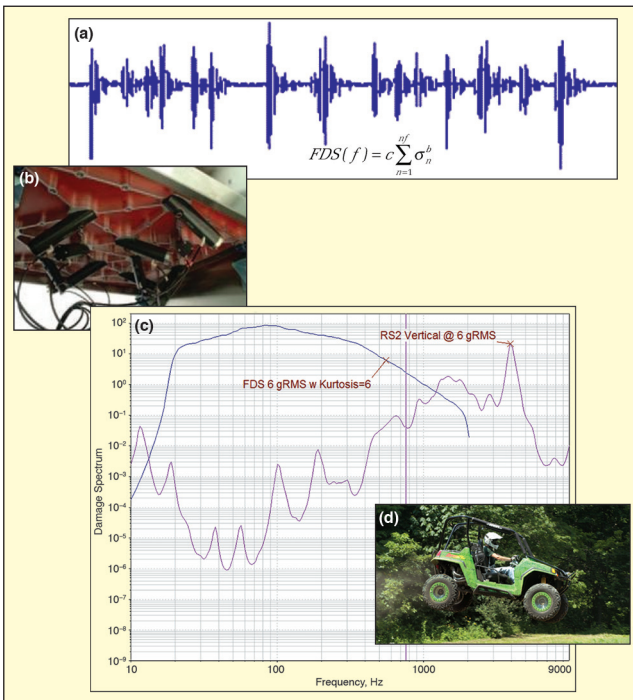


Figure 3. (a) typical RS machine time history; (b) underside of a repetitive shock test machine table; (c) FDS of 6  $g_{rms}$  ED shaker with Kurtosion = 6 and RS2; (d) typical end-use environment.

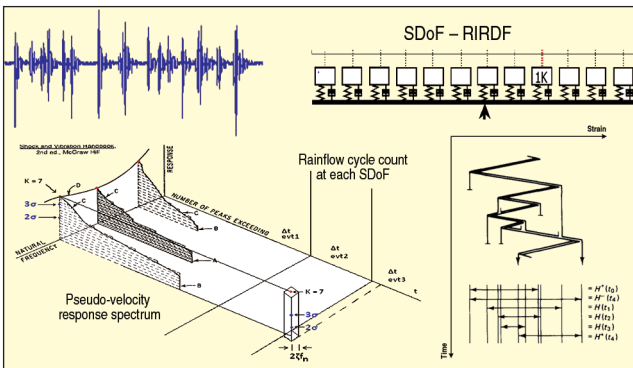


Figure 4. Graphical depiction of FDS and SDoF via RIRDF.

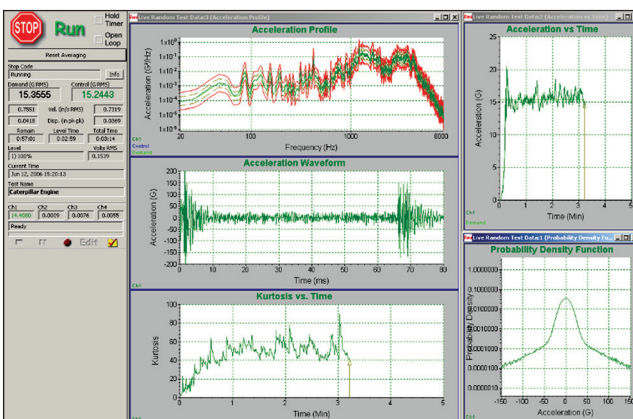


Figure 5. Diesel engine excitation at sensor location.

and resolution applied to *all* shaker types, end-use excitations and product responses – including acceleration and strain.

FDS as a summation:

$$FDS(f) = c \sum_{n=1}^{nf} \sigma_n^b \quad (1)$$

where  $n$  is the number of cycles counted by the rain-flow algorithm in the half-power bandwidth of each SDoF frequency, and total damage at every frequency is the sum of the individual damages

due to the cycles at that frequency, where the individual damage due to every cycle is exponential based on typical S-N curves.

### Insufficient Traditional Metrics

FDS accommodates greatly different peak probability distributions (PPDs). Figure 5 shows a diesel engine block sensor location under excitation of 15  $g_{rms}$  but with 15  $\sigma$  peaks to 237 g and a kurtosis of 55. Based on how a PSD is generated, excitations of different kurtosis produce an identical PSD and  $g_{RMS}$ . In short, traditional data processing under-represents the severity of the excitation in terms of damage.

- An FFT-generated PSD is neither mathematically nor practically valid for the non-Gaussian, non-stationary excitations of random shock (RS) machines.
- Because excitations can be non-Gaussian and non-stationary, a spectral shape and a  $g_{rms}$  level are not necessarily sufficient to describe an EUE, test spec, or product strength (operating and destruct limits) or service life.
- PSD is a statistical snapshot of a random process. The use of a PSD ( $g^2/Hz$ ) and  $g_{rms}$  lacks elements that correlate to failure mode, fatigue cycles, field exposure with peak amplitudes more severe than Gaussian.
- The PSD does not lead to the reliability and confidence numbers (MTBF, MTBUR) or % of life used that many seek from the HALT/HASS process.

### Fatigue Damage Spectrum

The Henderson-Piersol PSD-based DP(f) fatigue metric<sup>2</sup> showed no differences for different peak probability distributions (kurtosis), and did not accommodate the damage generated by RS machines and found in perhaps 40% of EUEs.

The essential requirement for FDS is a relationship to stress proportional to the velocity of the first bending mode per Gaberson<sup>4</sup> and cycle counting at high-frequency resolution. The PSD has neither a relationship to exposure time nor to stress cycles. A PSD of a three-second time history has the same information as a three hour or 37 week PSD. The  $g_{rms}$ , the root of the area under the PSD, is “non-unique,” requiring spectral shape and remains an average power of the excitation. For RS machines,  $g_{rms}$  is a set point for air pressure and has little or no relationship to damage imparted to fixtures, to UUT mounting points or to product responses.

Acknowledging the important differences in: 1) bandwidth over which ED and RS shakers have higher intensity; 2) the 3 or 6 DoF excitation versus 1 DoF; and 3) the dominance of the product response function. RS machines, ED and other shakers can be selected for products, assemblies and component interfaces that respond within the excited bandwidths. Because the FDS is basically a volume integral defined as in Figure 3, and the FDS plot points are essentially dimensionless, they can be summed and compared via ratio and difference.

To replace the filter function limitations of FFTs, FDS uses the SDoFs of the Smallwood ramp invariant recursive digital filter (RIRDF) front end for SRS. It is relevant for the transients of RS machines and valid for vibration generally. For the FDS, a rain-flow count of completed cycles at each 1/24th octave center frequency is used in lieu of the SRS peak-hold algorithm.

The flow diagram in Figure 6 was presented by John Van Baren and Tom Achatz previously<sup>6</sup> and in John Van Baren’s FDS article in this issue of *Sound & Vibration*.

To generate the FDS as a fatigue damage metric, the model requires an “ $m$ ” input, a generalized material constant equal to the negative slope of the material S-N curve. Also required is a  $Q$ , the quality factor of the product resonant response indicating the amplification of an input and yielding the effective half-power bandwidth. While these inputs are not as limiting as the Gaussian and stationary requirements for PSD and  $g_{rms}$ , they are still approximations. Their values and the FDS can be improved by knowing and mapping the materials and resonant frequencies of the UUT subassemblies.

### Test Set-Up

To allow and accommodate the beneficial variations in RS ma-

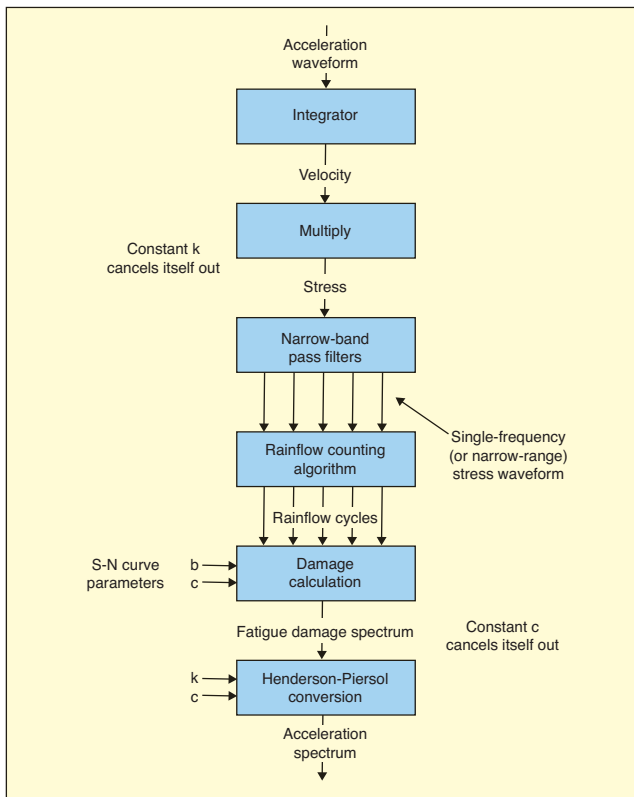


Figure 6. FDS calculation flowchart.

chine excitation due to hammer configurations, repetition rates and table dynamics, this exercise uses thin, resonant-rich plates on 1- and 2-inch stand-offs (Figure 7a) to emulate the equally compliant fixtures – long recommended for pneumatic RS machines and to act as simulated product mounting points.

Instrumentation (Figure 7b) was a pair of Vibration Research VR9504 controllers connected by Ethernet switch for 8-channel capability. Also used were VibrationVIEW, import, FDR and FDS software modules plus RecorderVIEW with waveform editor, and random control with Kurtosion.

### Test Plan and Data Collection

RS system set points of 6, 10, 20, 30 and 50  $g_{rms}$  were run for 5

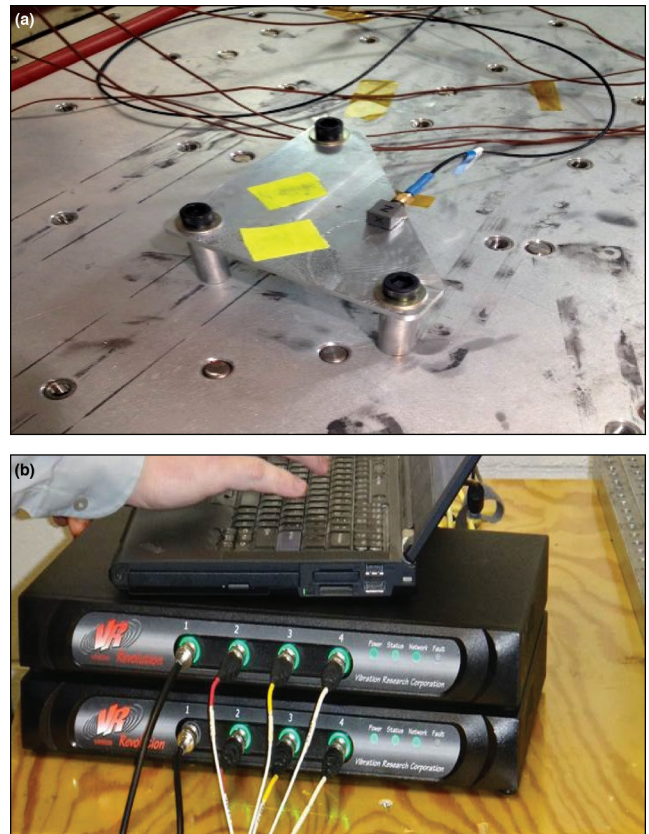


Figure 7a and 7b. RS shaker test setup fixture and VR data acquisition.

minutes each to record time histories adequate for PSDs, kurtosis development and fatigue damage exposure. For reference, results are compared at the same RS machine  $g_{rms}$  set points and results from ED shaker profiles. All recordings were at 100 kHz for analysis to 10 kHz.

Triaxial accelerometers on fixtures F1 and F2 recorded 5-minute time histories from two Dytran triax accelerometers and the control accelerometer from each RS machine used for closing the  $g_{rms}$  setpoint with air pressure. Table 1 summarizes Z (vertical) axis data as excitation and responses coincident with the RS machine control accelerometer. Time histories were streamed to the PC hard drive via VR9500s RecorderVIEW.

Table 1. Raw data summary; setpoint  $\pm$  peaks and Kurtosis; Z Axis Acceleration Readings on RS1, RS2 & RS3.

Machine	Setpoint Location	6 $g_{rms}$		10 $g_{rms}$		20 $g_{rms}$		30 $g_{rms}$		50 $g_{rms}$	
		$g_{rms}$	g pk +/-	$g_{rms}$	g pk +/-	$g_{rms}$	g pk +/-	$g_{rms}$	g pk +/-	$g_{rms}$ S	g pk +/-
RS 1 Z Axis	Fixture 1	14.26	443/442	32.41	262/279	37.82	422/434	103	981/727	N/A	N/A
	Fixture 2	19.38	399/350	40.05	241/230	75.2	447/452	105	784/822	N/A	N/A
	Kurtosis	K1= 8.36 K2= 6.53	K1= 4.32 K2= 3.66	K1= 6.73 K2= 3.3	K1= 3.96 K2= 4.16	K1= N/A K2= N/A					
RS 2 Z Axis	Fixture 1	10.35	117/118	19.9	217/213	39.7	467/402	64.22	602/636	113	1000/923
	Fixture 2	6.35	88/86	12.48	147/145	31.7	387/321	51.56	624/521	103	1115/902
	Kurtosis	K1= 14.5 K2= 14.2	K1= 8.24 K2= 9.19	K1= 6.17 K2= 6.02	K1= 5.28 K2= 5.91	K1= 5.01 K2= 5.63					
RS 3 Z Axis	Fixture 1	15.4	89/82	24.05	137/119	41.6	418/402	55.5	410/443	52.4	1073/854
	Fixture 2	25.1	140/140	41.7	206/210	73.7	406/399	102	637/560	156	830/776
	Kurtosis	K1= 3.11 K2= 3.29	K1= 3.09 K2= 3.03	K1= 3.39 K2= 3.03	K1= 3.17 K2= 3.04	K1= 3.8 K2= 3.06					
ED Shaker	Fixture 1	6.1	27/29	10	52/52	20	98/93	31	157/159	50.04	249/246
	Kurtosis*	K1 3		3		3		3		3	

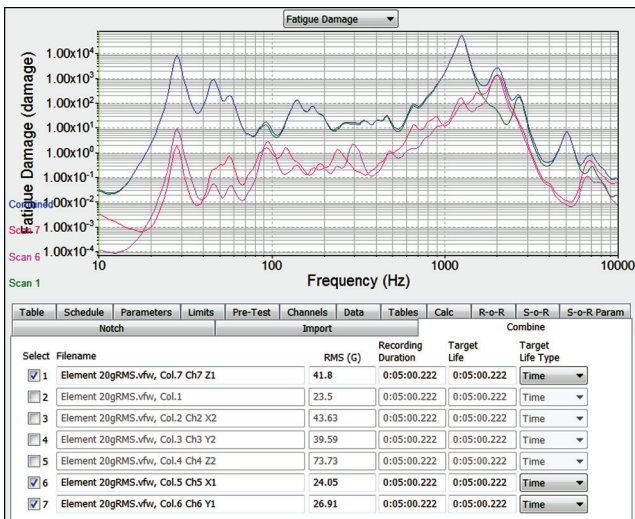


Figure 8. x, y and z fixture response contributions.

### Observations – Raw Acceleration Data

- The RMS levels of the RS machine excitations varied significantly from the desired control or set point.
- At 50  $g_{rms}$  set points, RS2 and RS3 machines over-ranged the triaxial response accelerometers.
- The positive and negative g peaks far exceeded the Gaussian range expected from a random excitation. Hence the RS or Random Shock designation for the machines
- For RS1 and RS2, kurtosis values exceeded the  $K=3$  of a Gaussian peak probability distribution (PPD).
- For RS3, the kurtosis values indicate a more Gaussian PPD and compared with the ED shaker at the same  $g_{rms}$  setpoints.
- The variations in responses of Fixtures 1 and 2 emphasize the critical consideration of the geometry and resonances of the unit under test (UUT) and location on the RS table.
- Kurtosis values are reasonably consistent between Fixtures 1 and 2 at each  $g_{rms}$  set-point level for all three machines.

From the same recorded data, Table 2 represent the FDS sums for the two fixtures on the RS2 machine. Again, the time was 5 minutes at each set point. Note that the F1 and F2 responses are nonlinear, with set points due to hammer repetition rates, table and fixture geometry and UUT structure and cycle counts of repetition rate harmonics.

### RS Machine Table Balance

The checked imports, Columns 5, and 6 in Figure 8, represent the horizontal plane (X and Y), and Column 7 is Z axis (vertical) showing the X, Y, Z balance at a single accelerometer location. RMS values between Z axis and X and Y axes vary by 1.6:1 while in terms of damage in Table 2, they vary from 100:1 to 1000:1. Should design engineers and physics-of-failure (POF) investigators have interest, the relative contributions of RS machine cross-axis, rotational inputs and product assembly responses can be quanti-

Table 2. FDS damage sums; RS2 input control and responses.

Setpoint	Fixture 1 with 1-inch stand-offs				Combined X1+Y1+Z1
	Control	X1-Ch2	Y1-Ch3	Z1 Ch4	
6 $g_{rms}$	110	125	64	74	263
10 $g_{rms}$	570	433	414	1175	2019
20 $g_{rms}$	6596	11321	8829	30559	50709
30 $g_{rms}$	36938	102661	62059	225923	390643
50 $g_{rms}$	116808	236245	236245	1799371	2172861
Setpoint	Fixture 2 with 2-inch stand-offs				X2+Y2+Z2
	Control	X2-Ch5	Y2-Ch6	Z2 Ch7	
6 $g_{rms}$	110	124	516	601	1242
10 $g_{rms}$	570	841	516	601	1959
20 $g_{rms}$	6596	30559	18180	10386	59126
30 $g_{rms}$	366938	147632	89835	252272	489740
50 $g_{rms}$	116808	587214	337916	2380313	3305443

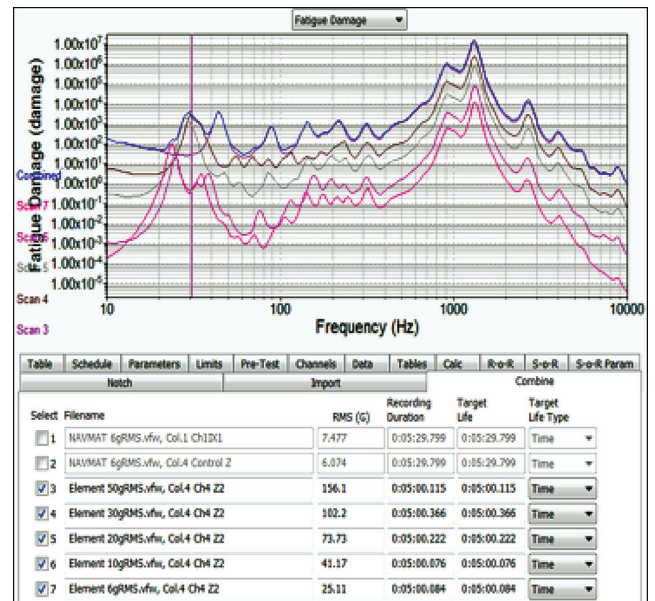


Figure 9. Step stress for 6, 10, 20, 30 and 50  $g_{rms}$  setpoints plus combined.

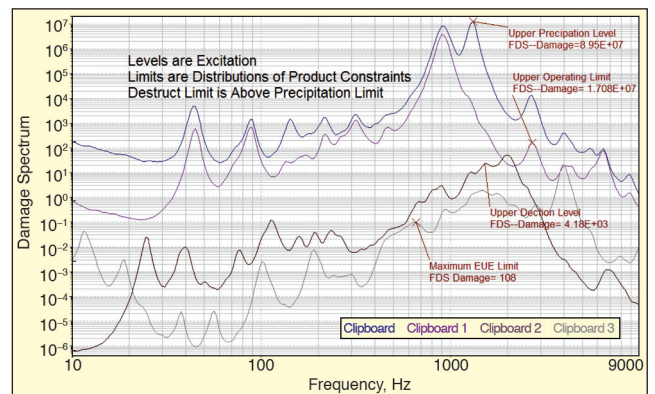


Figure 10. Precipitation and detection screen damage levels.

fied. The UUT response functions can be compared with the excitations to identify resonant response half-power bandwidths of potential damage. The FDS lends itself to combining traces as the global sum of the damage from 6, 10, 20, 30 and 50  $g_{rms}$  set points totaling 1,700,371, analogous to the  $g_{rms}$  power of a random test.

Figure 9 documents a HALT step-stress progression in terms of damage. Importing time histories for each step-stress level provides cumulative damage to the point of failure during the step-stress process and also the cumulative damage when step-stress is completed. It can be interpreted as a measure of product strength to compare with service life modeled in FDS from time-weighted environments a product experiences in the field.

In the HALT and HASS process, where intermittent failures can account for up to 70% of electronic malfunctions, powering and monitoring a product in concert with the cumulating FDS of the step-stress process can identify cumulative damage at which failure occurs via an alert of limits exceeded or test abort.

### Precipitation and Detection Levels

The step-stress process, dating back to ESS (Environmental Stress Screening) development, characterized a product by operating and destruct limits. The former being that exposure above which the product would cease to function properly, return to operating once the vibration is decreased or stopped. The destruct limit is the point at which the product ceases to operate at all and cannot recover and identify product design, component or manufacturing flaws. Superior to anecdotal observations of a  $g_{rms}$  level for a time period, Figure 10 shows how FDS can relate step-stress to the detection and precipitation screen in terms of damage.

Proof of screen and UUT exposure to HASS levels can be generated as a percentage of the FDS cumulative HALT damage achieved

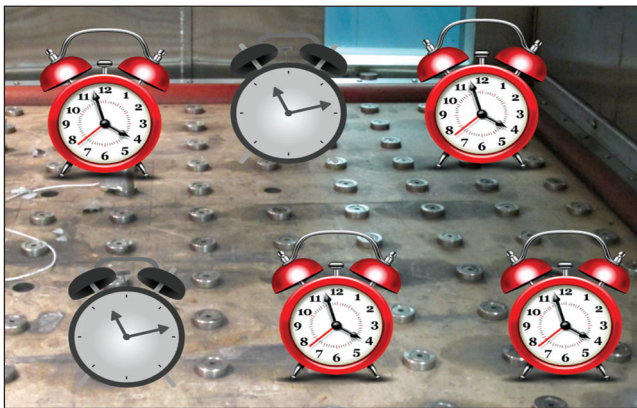


Figure 11. FDS fatigue clock for HASS accommodates table variances.

– or as a percentage of cumulative life modeled with FDS from multiple time histories and weighted exposures. Recall that each level is a distribution, not a discrete value.

### Managing Multi-UUT HASS

HASS severity and exposure can be scaled from the HALT FDS and damage sum. FDS also allows proof of screen (and HASS) as a percentage of HALT and of cumulative life model in terms of damage.

Implementing HASS in a production facility on large quantities is enhanced because the FDS serves as a fatigue clock. To accommodate variations in RS machine excitations and damage over the table, FDS is monitored at product/fixture or response locations. When a product or fixture location reaches the desired FDS level, products can be removed and replaced at appropriate times to achieve equal exposure as shown in Figure 11.

Prior to FDS, achieving equal damage was by guess or rule-of-thumb estimates (e.g., 15 minutes at 6  $g_{rms}$  set point), not pertinent to fatigue exposure.

### Comparison of Two RS Machines

The effects of the hammer fundamentals, their harmonics and table dynamics differ. Spectral coverage can be compared with product response functions to ensure resonances are excited. Both the  $g_{rms}$  power of the RS machine excitation *and* the peak accelerations in frequency bands contribute to the FDS. Gaberson<sup>4</sup> shows that velocity or pseudo velocity is a better indicator of damage being more closely related to stress and strain rate.

The fundamental hammer repetition rates and the FDS shift to higher frequencies with higher  $g_{rms}$  set points. The gaps in the spectra between the half-power bandwidths of the hammer fundamentals that should excite product resonances are at lower levels by orders of magnitude as shown in Figure 12. Compared with the RS2 shaker fundamentals in Figure 12, the RS3 fundamentals shown in Figure 13 are much more closely spaced at frequencies below 200-350 Hz, and the valleys between half power bandwidths of fundamental repetition rates are smaller, indicating better FDS spectral coverage.

As a tool for comparing RS machines, ED shakers, EUEs and test specifications, the damage sum is the volume integral described above and is the sum of all 1/24th octave points on the FDS broadband or selected product resonance bandwidths.

Figure 14, shows the FDS for RS2 and RS3 at 50  $g_{rms}$  set points with combined damage sums for both F1 and F2 and all three axes. Recall the FDS summation does include cross-coupling between axes but still presents a spectrum that can't be done with PSDs and  $g_{rms}$ . The UUT structural stiffness, resonant responses and damping remain variables in a more precise solution.

### FDS for Assembly Input and Response

The FDS depends on Miner's Rule to combine cycle-counted acceleration amplitudes using idealized "m" as a material constant from the slope of the S-N curve and Q as the quality factor. Once an assembly is targeted, FDS can be refined by selecting m and Q specific to assembly material and resonances at UUT loca-

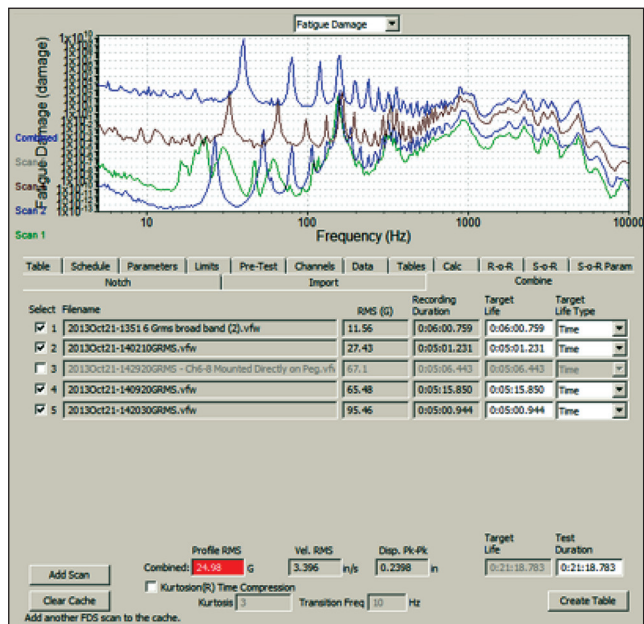


Figure 12. RS2 shaker FDS for 10, 20, 30 and 50  $g_{rms}$  set points.

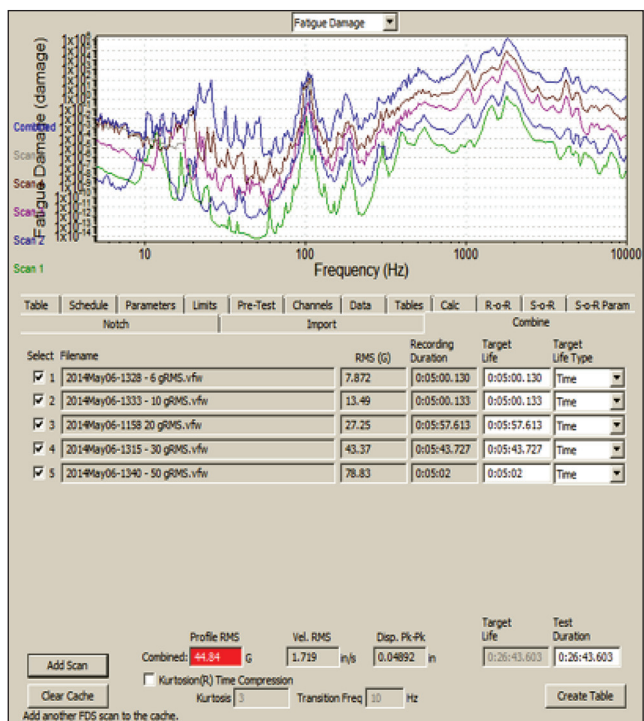


Figure 13. RS3 shaker FDS for 10, 20, 30 and 50  $g_{rms}$  set points.

tions. Figure 15 shows the FDS from the same time history and fixture location with different m and Q to reflect UUT structural resonances and materials. The concept of an FDS transmissibility (using bandwidth cursors marking the assembly half-power points) can quantify the damage sum for input and response for a specific resonance.

### Comparison of End-Use Environments

The FDS traces in Figure 16 reflect the mounting locations of nine avionics boxes in the cockpit of a military jet aircraft. Each FDS represents the cumulative damage for nine actual 1-hour flights. The differences in severity can be related to low MTBUR or failures by the suppliers of some of the boxes. One can also compare the expected service life and specifications to which the boxes were designed, qualified and tested by any HALT/HASS process.

Multiple time histories may be imported and combined. One advantage of the FDS is that imported files need not have the same sampling rate. In addition, each time history contributing to the

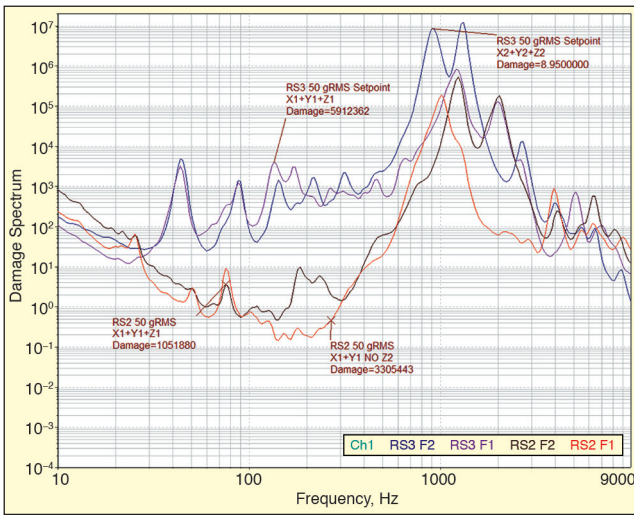


Figure 14. Shakers RS2 and RS3 with set points at 50  $g_{rms}$ : F1 and F2 with damage sums calculated.

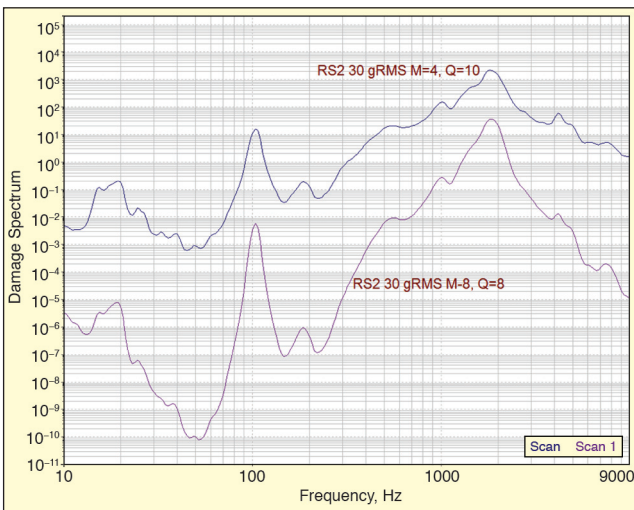


Figure 15. FDS for assembly input and response.

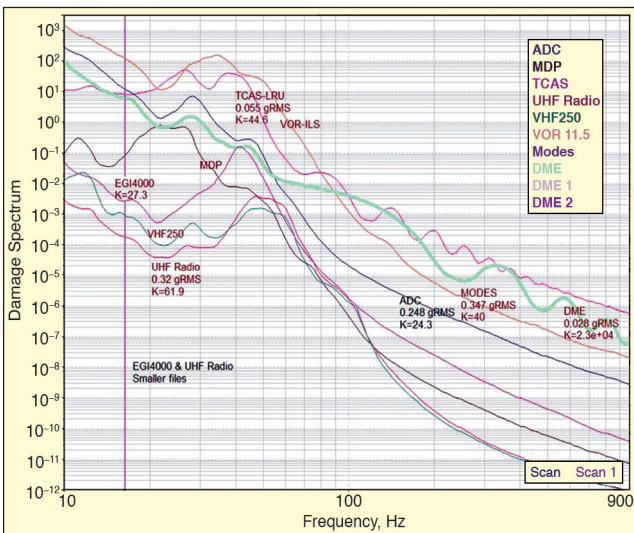


Figure 16. Comparison of avionics box and end-use environments.

cumulative FDS may be weighted by the desired time at level or number of passes (e.g. test track segments) for a total cumulative FDS.

The automotive assembly service-life FDS in Figure 17 is generated from multiple response time histories recorded and weighted for known vehicle use patterns. The process results in the compression of test time with damage equivalent to the service life.

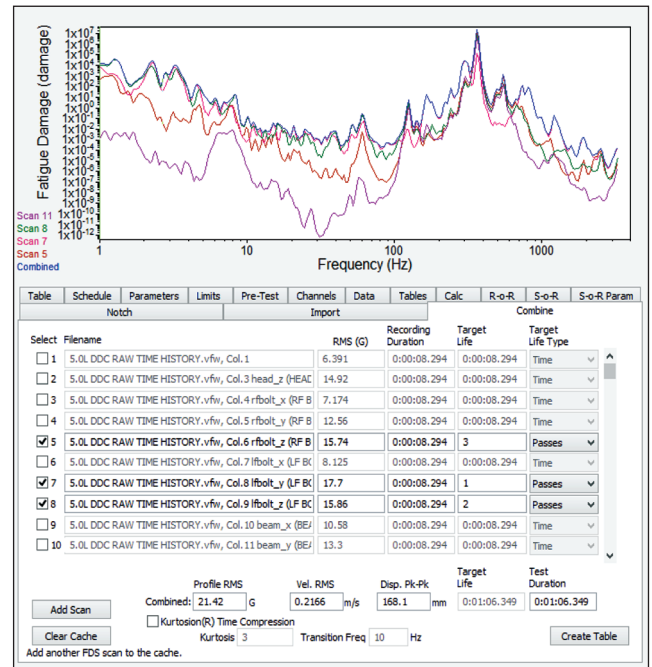


Figure 17. FDS combining multiple time histories defining service life.

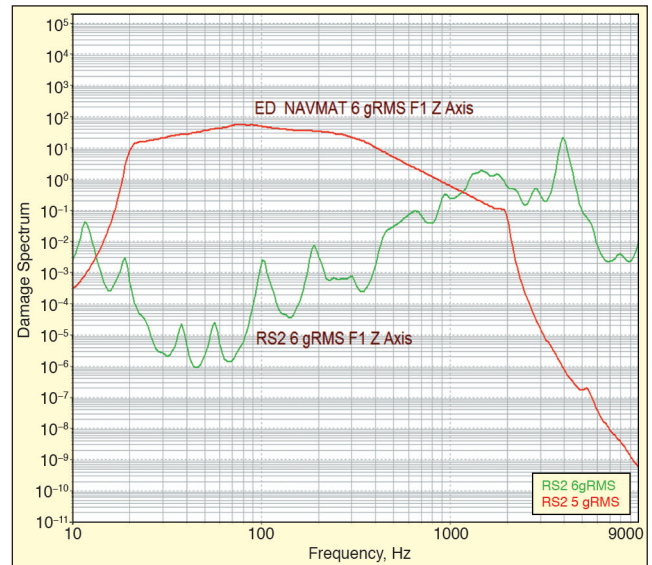


Figure 18. FDS comparison – RS machine and ED shaker at same set point.

### Comparison of HALT Margins and Product Service Life

Using FDS as an analyzer tool, the FDS of a modeled UUT service life can be directly compared with the result of the HALT step-stress, the fundamental limit of the design. The margins achieved, either in terms of damage sums for specific bandwidths or a broadband summation yield estimates for reliability prediction and analysis. One could conclude the UUT has been “HALTed” to multiple times of its projected life. FDS is thus a method for tracking the UUT performance in service.

### RS Machine and ED Shakers – FDS Comparison

Answering an often-asked question, Figure 18 shows the Z axis FDS comparison between an ED shaker running NAVMAT P9492 ESS guideline and an RS2, also at a 6  $g_{rms}$  set point, both for 5 minutes. Individual and combined X, Y and Z can be viewed as relative measures of cumulative three-axis damage – ignoring cross-coupling but giving credit for 3-DoF or 6-DoF contributions or response.

In addition to the minimally documented contributions of 3- or 6-DoF excitations of RS machines, ED frequency bandwidths excite UUT resonance bandwidths differently. ED shaker random excites all frequencies simultaneously in contrast to far fewer events in

lower frequency bands at RS machine repetition rates of 35 to 50 Hz. Above, the damage cross-over is approximately 1100 Hz. It is beneficial to view the UUT frequency response plots.

With  $m$ ,  $Q$  and the patented transition frequency of the VR Kurtosion, FDS can be used to tailor the test profile for an ED shaker used in the HALT/HASS role or optimizing replication of UUT service life. With FDS control, a breakpoint table and a PSD of equivalent damage are generated, describing a Gaussian random test incorporating damage of high kurtosis, non-Gaussian peaks and cycle counts from the time histories in 1/24th octave bands. Based on the peaks observed in the time histories accounted for in the FDS, the kurtosis may be re-introduced as a function of the Gaussian  $g_{rms}$  to modify the peak probability distribution generated to include recorded real-life peak accelerations.

For ED shakers, the comparison also allows a trade-off between Gaussian random with increased  $g_{rms}$  power to achieve peak accelerations of the EUE with lower  $g_{rms}$  plus Kurtosion, avoiding the possibility of overtesting. Product vibration specs could be augmented in terms of FDS – cumulative damage incorporating EUE kurtosis and cycle-counting. A Gaussian spectrum of equivalent damage can be generated from the FDS and Kurtosion reintroduced. The statistically more accurate random test improves test tailoring, eliminates the shortcomings of PSD and  $g_{rms}$  metrics and is applicable to EUE and all shaker excitations.

### Recommendations


- Use near real-time FDS updates to monitor and manage vibration tests on the basis of cumulative damage.
- Use FDS to provide an engineering-based metric for correlating the HALT/HASS process and the random shock machines with other excitations, tests and test objectives and reliability.
- Use FDS as an added criterion to vibration specifications to incorporate product service life, warranty and reliability considerations.
- Use the FDS tool to quantify simultaneous three-axis ED shaker effectiveness generally and when proposed for HALT processes on product not sufficiently stimulated by RS machines.
- RS machine XYZ can be characterized for balance at multiple locations, quantifying relative contributions of cross-axis inputs and rotations, fixture design and a rough estimate of cumulative damage. Also benchmark performance over time.

### Conclusions

These data from and the use of FDS lead to a better understanding of what should be expected from the  $g_{rms}$  set point of an RS machine. The set point does not relate to the  $g_{rms}$  level generated by the RS machine and, more importantly, does not relate to the damage imparted to the UUT. FDS plots are spectra, cumulative volumes providing a global damage metric for broadband or for selected bandwidths.

The FDS techniques illustrated here are applicable to defining a product strength as a function of desired service life, comparing with HALT step-stress levels, and relating to traditional ED shaker tests and end-use environments.

### References

1. Svensson, T. and Torstensson, H.O., "Utilization of Fatigue Damage Response Spectrum in the Evaluation of Transport Stresses," IES 1993 ATM, May 2-7, Las Vegas, NV.
2. Piersol, A. G., Henderson, G. R., "Fatigue Damage Related Descriptor for Random Vibration Test Equipment," *Sound & Vibration*, Vol. 29, No. 10, pp. 20-24.
3. Van Baren, John and Phillip, "Kurtosion™ – Getting the Kurtosis into the Resonances," SAVIAC, 2007.
4. Gaberson, Howard A., "Pseudo-Velocity Shock Spectrum Rules for Analysis of Mechanical Shock," IMAC, 2007.
5. Smithson, Stephen A., "A Viewpoint on Fatigue Metrics – Benefits for HALT, HASS and More," 10th Annual Workshop on Accelerated Stress Testing and Reliability, Chicago, October 2004.
6. Achatz, Thomas M., and Van Baren, John G. , "Using Fatigue Damage Spectrum for Accelerated Testing with Correlation to End-use Environment," Accelerated Stress Testing and Reliability Workshop, St. Paul, MN, October 10-12, 2014. 

The author can be reached at: [reps@smithson-associates.com](mailto:reps@smithson-associates.com).